Inverted U-shaped brain development of cognitive control across the human lifespan

Zhenghan Li[1,2,3,4], Isaac T. Petersen[5], Lingxiao Wang[6,7,3], Joaquim Radua[8,9,10], Guochun Yang[5,11,4*], Xun Liu[4,12]

[1] Institute of Brain Science and Department of Physiology, School of Basic Medical Sciences, Hangzhou Normal University, Hangzhou, China

[2] Zhejiang Philosophy and Social Science Laboratory for Research in Early Development and Childcare, Hangzhou Normal University, Hangzhou, China

[3] Zhejiang Key Laboratory for Research in Assessment of Cognitive Impairments, Hangzhou, China

[4] Key Laboratory of Behavioral Science, Institute of Psychology, Chinese Academy of Sciences, Beijing, China

[5] Department of Psychological and Brain Sciences, University of Iowa, Iowa City, IA, USA

[6] Centre for Cognition and Brain disorders, The Affiliated Hospital of Hangzhou Normal University, Hangzhou, Zhejiang Province, China

[7] Institute of Psychological Science, Hangzhou Normal University, Hangzhou, Zhejiang Province, China

[8] Institut d'Investigacions Biomèdiques August Pi i Sunyer (IDIBAPS), CIBERSAM, University of Barcelona, Barcelona, Spain

[9] Institute of Psychiatry, Psychology and Neuroscience, King's College London, London, United Kingdom

[10] Department of Clinical Neuroscience, Karolinska Institute, Stockholm, Sweden

[11] Cognitive Control Collaborative, University of Iowa, Iowa City, IA, USA

[12] Department of Psychology, University of Chinese Academy of Sciences, Beijing, China

*Correspondence: guochun-yang@uiowa.edu

Abstract

Cognitive control, a crucial brain function for goal-directed human behavior, exhibits dynamic changes throughout the lifespan. However, the specific age-related alterations of brain activities related to cognitive control remain under-investigated. To address this gap, we conducted a comprehensive meta-analysis of 107 neuroimaging studies using conflict tasks, encompassing 3,153 participants whose age spanned from 5 to 85 years old. Using the seed-based effect size mapping and meta-regression approaches, we unveiled brain regions with activities exhibiting an inverted U-shaped developmental trajectory within cognitive control network, peaking between the ages of 24 and 41 years. Conversely, regions associated with the dorsal attention network displayed relatively more stable activity across the lifespan. Additionally, we observed evidence of greater left laterality of brain activities in both the youth and elderly. These results highlight the inverted U-shaped trajectories in cognitive control brain activities, while also revealing the heterogeneity in brain development for different regions.

Introduction

The cognitive abilities of human beings dynamically change throughout the entire lifespan, experiencing rapid development in the early stages, and gradual decline in the later period of life. As one of the most essential cognitive functions, cognitive control is a fundamental component of advanced intelligence that distinguishes humans from other species[1]. Cognitive control refers to the cognitive processes that enable individuals to manage and regulate their attention, thoughts, and actions, which plays a vital role in goal-directed behavior, allowing us to focus on the target and ignore distractors[2,3]. For instance, cognitive control enables us to concentrate on reading in a library despite the presence of people chatting nearby. While young adults typically maintain a sufficient level of cognitive control as required, the youth

(including children and adolescents) and elderly individuals may struggle with behavioral problems because of their lower level of cognitive control[4]. For instance, children and adolescents may suffer from attentional deficits and have risk-taking/addiction issues due to underdeveloped cognitive control system[5,6], whereas elders may have difficulty focusing on target information as a result of decay in cognitive control[7]. Understanding how cognitive control changes over the lifespan can elucidate the developmental principles of cognitive control and provide valuable insights for the education of school-age children and interventions for elderly individuals at risk of cognitive decline.

Researchers have generally proposed that the cognitive control ability follows an inverted U-shaped trajectory across the lifespan[4,8,9], though the precise developmental courses may vary across different aspects of cognitive control (e.g., flexibility, working memory, etc.)[10]. Specifically, infants initially possess limited cognitive control that gradually develops as the brain anatomy matures. These functions continue to progress, reaching their peaks during young adulthood and maintaining relative stability until middle age, after which they begin to decline in elderly age[11]. This inverted U-shaped trajectory has been supported by ample behavioral evidence. For example, there were studies that found a clear U-shape trajectory of conflict cost (measured by increased reaction time in incongruent compared to congruent conditions) with age[10,12]. Recent large-cohort studies have also found that grey and white matter volumes across all brain regions exhibit inverted U-shaped trajectories with age[13,14], potentially providing the anatomical foundations for the cognitive control developmental trajectory. Consistently, the gray matter volumes of the frontal and parietal regions, which are essential in cognitive control tasks[15], have also been found to increase during adolescence and atrophy in early elderly age[16]. However, it remains largely unknown how brain activities during the performance of cognitive control tasks change over the lifespan.

Previous research has primarily focused on brain activities in either youths or elderly adults, rather than examining changes across the entire lifespan. Children and adolescents are often found to have lower brain activity than young adults in frontoparietal regions[17,18]. For example, Bunge et al.[18] found that children aged 8−12 years had limited activation of frontal brain regions compared to young adults during tasks involving interference suppression and response inhibition, suggesting an immature cognitive control system. However, brain activity differences in elderly adults as compared to young adults during cognitive control tasks have not been consistently reported[9]. Some studies have found that elderly adults have lower neural activity in frontoparietal regions than young adults[19,20], possibly because elderly adults may be unable to engage in an equal level of control-related activity due to functional decline. On the other hand, other studies have found that elderly adults may exhibit greater brain activity in frontoparietal regions than young adults[21,22], possibly because they have recruited additional brain regions to compensate for their decreased efficiency in utilizing control resources. As a result, it is difficult to draw a clear conclusion about how brain activities related to cognitive control change across the entire age range.

One direct way to test the trajectory of brain activation related to cognitive control is to conduct a large cohort of neuroimaging study with participants covering a wide age range. To the best of our knowledge, such studies have not yet been conducted. An alternative approach is to utilize meta-analyses to combine the results of existing studies targeting different age groups. Compared to the large cohort studies, meta-analyses are more readily available and resource-saving. In addition, meta-analyses show several advantages over individual studies. By combining results from various studies, meta-analyses can increase the statistical power and generalizability of the findings and thus result in more precise conclusions. Meta-analyses can also reduce the heterogeneity and bias that may exist in individual studies because of different methods, populations, or confounding variables[23].

114 Importantly, meta-analyses can reveal patterns or trends that may not be immediately
115 evident in individual studies, such as nonlinear effects or interactions[23]. There have
116 been several neuroimaging meta-analyses that attempted to examine the effect of age
117 on cognitive control[20,24,25], but a few limitations prevent them from appropriately
118 answering questions about the developmental trajectory of cognitive control functions.
119 These limitations include not covering the full range of age across the lifespan[20,24], or
120 having too few studies in some age ranges (e.g., elderly adults[25]). In addition, these
121 studies have primarily focused on the spatial convergence and/or diversity of reported
122 coordinates across different age ranges using methods like the activation likelihood
123 estimation (ALE), which provides limited insights into developmental trajectory of
124 activity strength. Although a few studies have attempted parametric meta-regression
125 with the seed-based *d* mapping (SDM) approach to examine the age-related
126 differences in cognitive control[24,31], they have been constrained by utilizing linear
127 models that may overlook non-linear trajectory patterns, such as the inverted
128 U-shaped trend.

129 The goal of this study is to reveal the developmental trajectory of brain activities
130 responsible for cognitive control across the lifespan. Instead of conducting a
131 comprehensive meta-analysis encompassing various aspects of cognitive control such
132 as working memory, inhibitory control, and conflict processing, we choose to focus
133 on conflict processing as an indicator of cognitive control for several reasons. First,
134 conflict processing reflects the ability to maintain a goal in mind while avoiding
135 distractions, which is a fundamental aspect of cognitive control[2]. Second, the
136 mechanisms underlying conflict processing in young adults are relatively well-known,
137 with the frontoparietal and cingulo-opercular networks repeatedly reported as the
138 most involved brain regions[15,26], providing a baseline reference for our study. Third,
139 conflict tasks with neuroimaging data have been widely applied to both younger and
140 elderly groups, making a systematic meta-analysis feasible. Lastly, conflict processing
141 exhibits a clearly defined congruency effect (i.e., the contrast between incongruent

142 and congruent/neutral conditions), which enables us to conduct effect-size based
143 meta-analyses. Including other sub-processes of cognitive control may introduce
144 heterogeneity and make the effect sizes incomparable.

145 Based on previous research, we hypothesized that brain activities related to
146 cognitive control increase rapidly from childhood to adolescence, reach a peak in
147 young adulthood, and then gradually decline with increasing age, following an
148 inverted U-shaped trajectory.

149 **Results**

150 The present study incorporated a total of 107 studies, where the average age of
151 participants in each study spanned from 8 to 74 years. Individual participants within
152 these studies ranged from 5 to 85 years old. To ensure the representativeness of the
153 average age in each study, we excluded individual studies with relatively large age
154 ranges (e.g., 19−64 years). The supplementary Table S1 describes the detailed
155 information for the included studies.

156 **Regions related to cognitive control identified by both ALE and SDM**

157 To enhance the replicability and robustness of our finding and enable direct
158 comparison with our previous study[15], we conducted the mean analysis across all
159 studies with the ALE and SDM approaches separately. First, we performed the single
160 dataset analysis with the GingerALE software to explore the consistently of brain
161 regions reported in all the included studies. Results showed significant activation in
162 the frontoparietal regions, including the left dorsolateral prefrontal cortex (dlPFC),
163 left frontal eye field (FEF), right inferior frontal gyrus (IFG) and bilateral superior
164 parietal lobule (SPL); the cingulo-opercular regions, including the pre-supplementary
165 motor area (pre-SMA) and right insula; and other regions, including bilateral inferior
166 temporal gyri (ITG) and left thalamus (Figure 1A and supplementary Table S2).

Second, we calculated the average brain activation based on the effect sizes reported in all studies using the SDM with permutation of subject images (SDM-PSI) software. Similar to the ALE results, we found significant activity in the frontoparietal regions (bilateral IFG, right FEF, and bilateral SPL), the cingulo-opercular regions (left anterior cingulate cortex (ACC)), and other regions like bilateral ITG, right caudate nucleus (CN), right thalamus, and right cerebellum (CBL) (Figure 1B and supplementary Table S3). Despite their methodological distinction, that is, the SDM approach additionally incorporates the statistical values of brain activation compared to the ALE, these two approaches yielded very similar results (Figure 1C), both replicating our previous study including only the young adult studies[15]. The count of voxels revealed that the overlapped area (10,749 voxels) accounted for 71.1% of the regions from the ALE analysis (15,113 voxels), and 53.4% of the regions from the SDM analysis (20,129 voxels). This result also suggested that SDM analysis showed a greater sensitivity than the ALE analysis under the common threshold ($p < 0.001$, cluster $\geq$ 10 voxels).

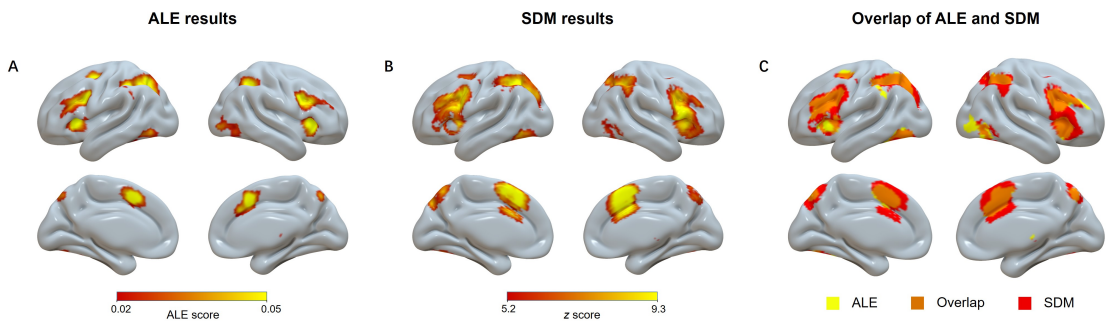

Figure 1. Overview of significant clusters across all studies regardless of age in the ALE meta-analysis (A), the SDM meta-analysis (B), and their overlap (C). ALE = activation likelihood estimation; SDM = seed-based *d* mapping.

Detecting inverted U-shaped trajectories

To identify the possible brain regions following the inverted U-shaped developmental trajectory, previous studies have adopted quadratic and cubic functions[27-29]. However, there could be shapes that cannot be captured by the above functions, such as

scenarios where one of the youth/elderly groups demonstrates an approximate level of activity to the young adult. To fully identify regions showing rising and/or fall trajectories, we conducted a contrast analysis between the young adult (20−44 years) and the other age groups with the SDM-PSI. To capture another possibility that brain activity of the youth/elderly groups exhibits opposite patterns compared to young adults, we conducted a linear analysis (see Supplementary Note S1). We identified greater activity in young adults compared to other age ranges in the frontoparietal regions, including bilateral IFG, right IPL, left SPL and left precuneus; the cingulo-opercular regions, including left pre-SMA and left anterior and posterior insula; and other regions, including bilateral CN, left anterior thalamic projections (ATP), right middle temporal gyrus, left CBL, left supramarginal gyrus (SMG), and left superior temporal gyrus (Figure 2 and Table 1). Notably, none of the clusters showed significant publication bias based on Egger's test ($p > 0.05$), and they all showed low between-study heterogeneity ($I^2 < 25\%$). This indicates that the observed results are not likely influenced by biased reporting or substantial variability in the included studies.

In addition, we failed to observe any region showing lower activity in young adults than the other ages (i.e., the upright U-shaped trajectory), even when we used a very lenient threshold ($p < 0.05$, uncorrected).

Fitting the inverted U-shaped trajectories with the generalized additive model (GAM)

Results from the GAM are shown in Figure 2 and supplementary Table S4. For each region, the GAM could fit the data significantly with a smooth curve, Fs > 10.0, ps < 0.001, with degrees of freedom varying from 3.7 to 7.1. Peak ages of the inverted-U shaped trajectories were between 24.6 and 40.7 years.

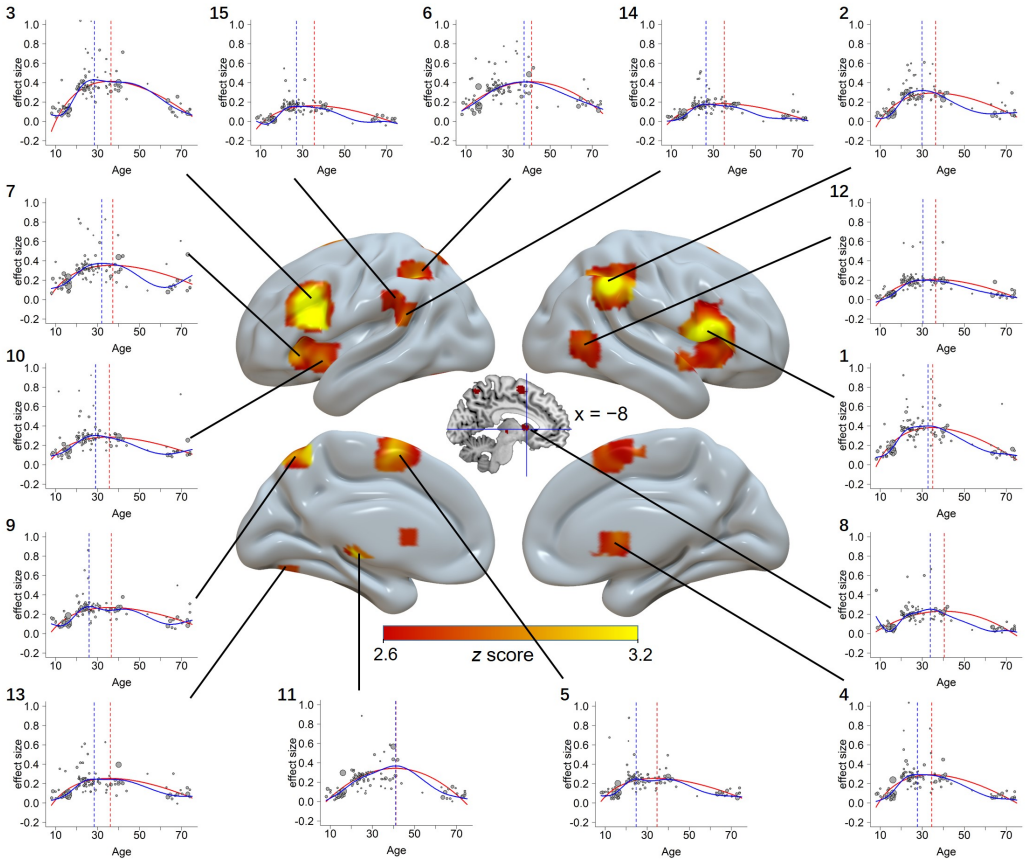

Figure 2. Brain regions showing inverted U-shaped trajectory patterns. Scattered plots are the effect size as a function of age, with curves fitted by GAM (blue color) and the best simplified model (red color). Dashed vertical lines show peak ages estimated from GAM (blue) and simplified model (red). The sizes of the scattered dots show the square root of model weights (1/variance) for each study. The numbers at the up-left corner of each plot correspond to the orders in Table 1. 1: right inferior frontal gyrus, 2: right inferior parietal lobule, 3: left inferior frontal gyrus, 4: right caudate nucleus, 5: left pre-supplementary motor area, 6: left superior parietal lobule, 7: left anterior insula, 8: left caudate nucleus, 9: left precuneus, 10: left posterior insula, 11: left anterior thalamic projections, 12: right middle temporal gyrus, 13: left cerebellum, 14: left supramarginal gyrus, 15: left superior temporal gyrus.

Model simplification of the inverted U-shaped trajectories

Considering the GAM may overfit the data, we fitted the results with simpler models commonly adopted in developmental literature[27-29], including the quadratic, cubic, square root and quadratic logarithmic models, and estimated the goodness of fit by comparing their Akaike information criterion (AIC) (see section "Model simplification and model comparison" in Methods). Weights of each model based on

AIC values for each region are presented in supplementary Table S5. Results showed that the quadratic model provided the best fit for capturing the age-related changes in left SPL and left ATP, while the square root model demonstrated the best goodness of fit for all the other regions. We also calculated the peak age for each region based on the optimal model, and results showed that the peak ages ranged from 34.1 to 40.8 years. In addition, we found the peak ages obtained from the above optimal model (i.e., square root or quadratic models) and the GAM are consistent, $r = 0.86$, $p < 0.001$. The detailed results of the optimal model fitting are shown in Figure 2 and supplementary Table S6.

Regions showing the quadratic and square root trajectories

Based on model comparisons, we found that the quadratic and square root models provided the best goodness of fit for the age-related change of the brain activities. To supplement the inverted U-shaped results from the contrast analysis, these two models were then submitted to whole-brain meta-regression analyses in SDM-PSI.

By fitting the activation over the whole brain using the quadratic model, we found five significant brain regions, including the bilateral IFG, right IPL, right SMG, and left ATP (Figure 3A and supplementary Table S7). Similarly, the square root model revealed seven significant brain regions, including the bilateral IFG, left IPL, right SMG, left SMA and bilateral ATP (Figure 3B and supplementary Table S7). These regions exhibited considerable overlap with the results obtained from the contrast analysis, although featuring fewer and relatively smaller significant clusters (Table 1 and supplementary Table S7). These results further supported the existence of the inverted U-shaped regions we initially identified, while also indicating that the contrast analysis exhibited a higher sensitivity compared to these functions.

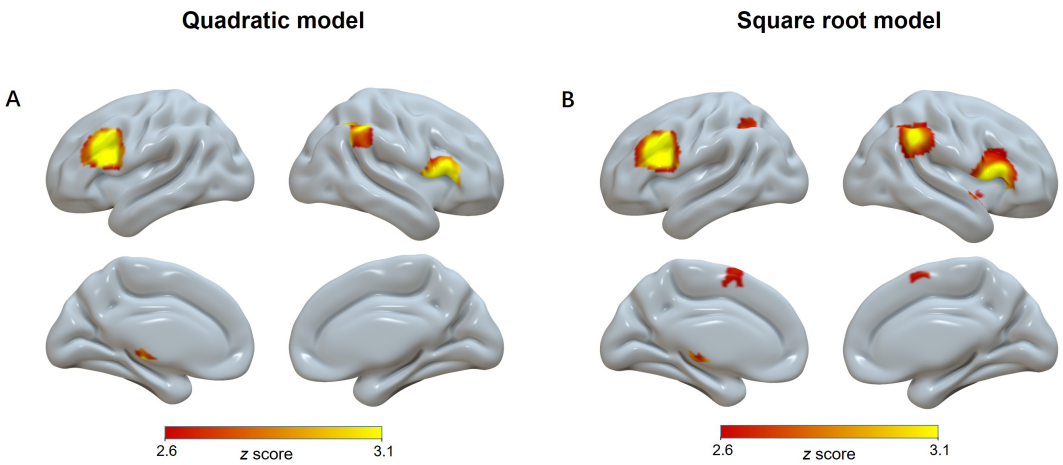

Figure 3. Significant clusters (voxel-wise FWE-corrected, $p < 0.001$, voxels ≥ 10) showing quadratic pattern (A) and square root pattern (B) with age in the model fitting.

Dissociated brain networks with distinct developmental trajectory

We note that the inverted U-shaped regions (Figure 2) constitute only part of the cognitive control-related regions (Figure 1). Because no upright U-shaped regions was observed, the remaining regions should show no difference between young adults and other ages, or a flat trajectory in other words. We used the results from the mean SDM analysis (see section "Regions related to cognitive control identified by both ALE and SDM") as the mask and replotted the results of the contrast analysis with two different thresholds (Figure 4). Results showed that the distribution of inverted U-shaped regions was more consistent with the cognitive control network, and the distribution of non-inverted U-shaped regions was more closely related to the dorsal attention network, based on the Yeo's 7-network atlas[30] (Figure 4B). The count of voxels revealed that a larger portion of the inverted U-shaped regions overlapped with the cognitive control network (1,814 voxels) than with the dorsal attention network (894 voxels). Conversely, a larger portion of the non-inverted U-shaped regions overlapped with the dorsal attention network (3,171 voxels) than with the cognitive control network (2,393 voxels).

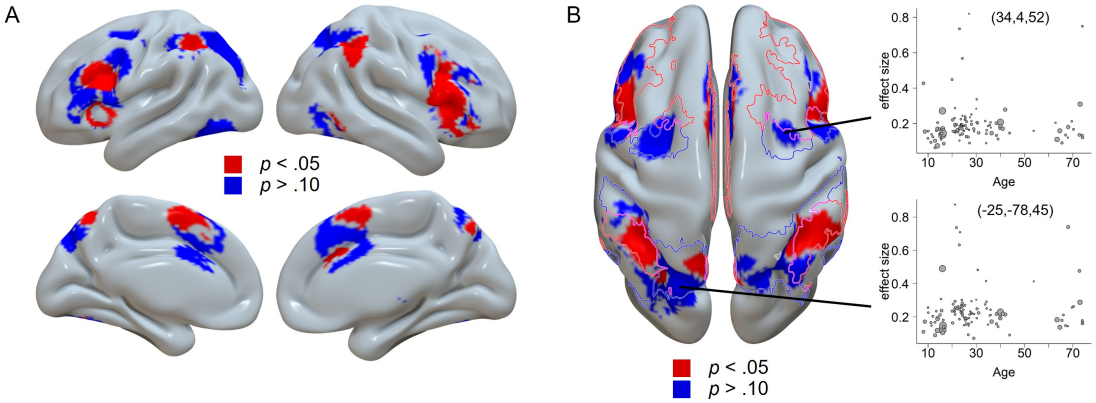

Figure 4. Dissociated brain regions based on their trajectory patterns. A) The regions following inverted U-shaped trajectories (red color) and non-inverted U-shaped trajectories (blue color). B) The axial view of the same results. The border lines display the cognitive control network (red) and dorsal attention network (blue) from Yeo's 7-network atlas[30]. The two scatter plots show two example regions showing the non-inverted U-shaped trajectory.

To further investigate the potential functional difference between the two sets of brain regions, we decoded the related terms with the NeuroSynth decoder[31] (see section "Neurosynth decoding analysis" in Methods). Results showed that the inverted U-shaped regions were related to the term "cognitive control" with a relatively high correlation (r = 0.196), but were less related to "attention" (r = 0.064). On the other hand, the non-inverted U-shaped regions were related to the term "attentional" (r = 0.252) but were less related to "control" (r = 0.056) (supplementary Table S8). This result further validated that the inverted and non-inverted U-shaped regions are specifically involved in cognitive control and attention, respectively.

To provide additional insight into the non-inverted U-shaped trajectory, we specifically chose two coordinates for analysis (Figure 4B), one ([34, 4, 52]) representing a peak region from the average brain activity analysis using SDM-PSI (supplementary Table S3), and the other ([−25, −78, 45]) representing a region displaying a null effect from the contrast analysis with p between 0.49 and 0.51, indicating a trajectory that does not align with either an inverted or upright U-shaped pattern. The GAM analysis showed that neither coordinate could be adequately fitted by a smoothed curve, with ps > 0.16. These results elucidate that the non-inverted

298 U-shaped regions exhibit relatively stable brain activities across the lifespan
299 compared to regions showing inverted U-shaped patterns.

300 **U-shaped trajectory of the laterality**

301 We also tested how the laterality of the brain activity changes with age (see section
302 "Laterality analysis" in Methods). We first modeled the laterality trajectory using the
303 GAM. Results showed a significant model fitting, $F(4.1, 5.1) = 2.47$, $p = 0.041$. The
304 estimated valley age was 27.7 (Figure 5A, blue color). Moreover, we fitted the data
305 with the four simplified models (i.e., the quadratic, cubic, square root, and quadratic
306 logarithmic models). The results showed that a quadratic logarithmic function
307 provided the best goodness of fit, with the $\beta_{\log(\text{age})} = -2.38$ and $\beta_{(\log(\text{age}))^2} = 0.35$, both
308 ps < 0.001. The estimated valley age was 28.8 (Figure 5A, red color). An upright
309 U-shaped trajectory indicated the youth and elderly adults were more left lateralized
310 across the whole brain. This pattern could be illustrated by the brain map estimated
311 with voxel-wise laterality calculation (Figure 5B). In addition, the prefrontal regions
312 appeared to be the major area driving the U-shaped trajectory, with the youth and
313 elderly adults more left lateralized than the young adult group.

314 Our previous study[15] showed that the semantic conflicts (e.g., Stroop) are
315 left-lateralized and the response conflicts (e.g., Simon) are right lateralized. To test if
316 the upright U-shape of laterality trajectory was affected by the type of conflict tasks
317 involved, we conducted an additional analysis. We only included the semantic type
318 (coded as 1) and the response type (coded as −1) in this analysis (102 studies), and
319 added the conflict type as well as the interaction term between the age predictor (i.e.,
320 logarithm of age) and conflict type to the above mentioned quadratic logarithmic
321 model. Results showed that the age effects remained significant for both $\beta_{(\log(\text{age}))}$ and
322 $\beta_{(\log(\text{age}))^2}$ (ps < 0.05), but neither conflict type nor the interaction term was significant
323 (ps > 0.76). This ruled out the possibility that the laterality trajectory results were

driven by different conflict types.

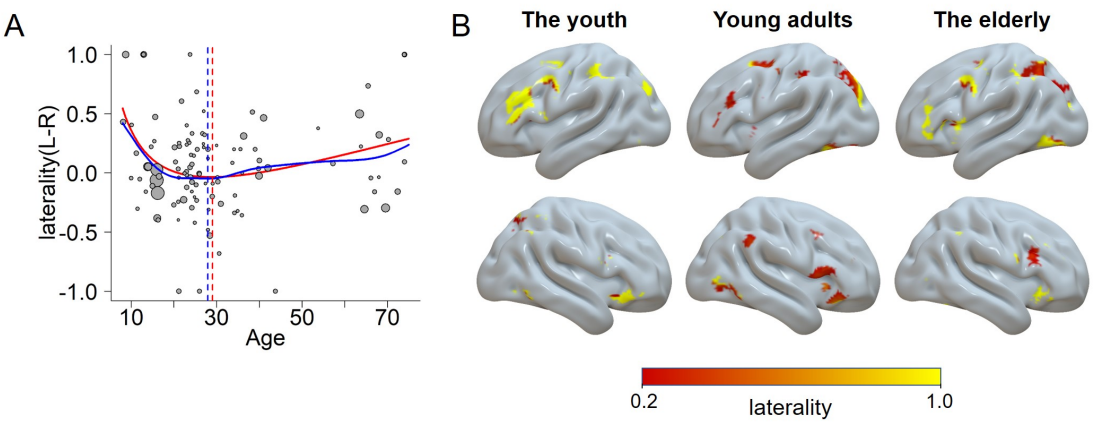

Figure 5. The laterality as a function of age. A) The trajectory fitted with a quadratic logarithmic model (red) and the GAM (blue). Higher values mean more left-lateralized and lower values mean more right-lateralized. B) Visualization of the laterality for each group. Regions in the left hemisphere show the left lateralized regions, and vice versa.

Discussion

The objective of this meta-analysis was to investigate the age-related changes in brain regions associated with cognitive control across the lifespan. Using data from 107 studies that encompassing participants aged 8 to 74 years on average, we examined how the activities of cognitive control regions vary with age. Our analyses yielded three primary findings: 1) The activity within the cognitive control network regions displayed a progressive rise from early childhood to young adulthood, reaching its peak between the ages of 24−41 years, and decline in elderly adulthood, demonstrating inverted U-shaped patterns; 2) In contrast, regions within the dorsal attention network exhibited similar activity levels across different age ranges, suggesting relative stability throughout the lifespan; 3) Both the youth and the elderly groups demonstrated a greater left laterality of brain activity compared to the young adult group, indicating hemispheric differences in cognitive control processes. These results provide strong evidence for the existence of cognitive control regions

exhibiting inverted U-shaped trajectory, and also show the heterogenous developmental trajectories for different brain regions.

The main result is that a wide range of cognitive control regions follow inverted U-shaped developmental trajectories, with no regions showing upright U-shaped or linear trajectories (supplementary Note S1). The greater activation in the cognitive control network among young adults compared to youth and elderly adults is consistent with the idea that the cognitive control system is most effective in young adulthood. This finding supports the notion that cognitive control abilities may not be fully developed in children and may decline in the elderly, providing a potential explanation for the superior performance of young adults on cognitive control tasks[11]. The inverted U-shaped trajectories of cognitive control regions are also consistent with the idea that cognitive control is an important aspect of fluid intelligence, which is known to peak in early to mid-adulthood and decline with age[4]. Hence, our findings may reflect the general rise-and-fall patterns in the higher-order brain functions.

The inverted U-shaped trajectory observed in cognitive control regions may be explained by two underlying factors. First, it may reflect the well-documented structural changes that occur in these regions across the lifespan, which include synaptic pruning, myelination, cortical thinning, and white matter maturation[13,14]. These changes can affect the efficiency and connectivity of neural circuits within the cognitive control network[8,32]. Second, the inverted-U shaped trajectory may also arise from functional changes resulting from the modulation of neurotransmitters, hormones, and environmental factors[33]. For example, the density of dopamine receptors increases during adolescence and young adulthood and subsequently declines with age[34]. Together, these age-related structural and functional changes may contribute to the developmental trajectory of cognitive control regions. Understanding developmental changes in brain structure and function is critical for developing interventions and treatments aimed at improving cognitive control abilities across the lifespan.

The present results further revealed that the inverted U-shaped developmental trajectories of cognitive control regions are not uniform. The GAM fitting results (Figure 2, supplementary Table S4) showed that the subregions exhibited varying degrees of modulation effects by age. Moreover, the model simplification demonstrated different underlying trajectory curves, with most regions showing a skewed shape that could best be fitted with a square root model, except that a small number of regions showing a symmetric quadratic shape. The quadratic developmental trajectory has been well-documented in previous studies[13,27,29,35], while the application of the square root model has been relatively rare[36]. The square root model can better capture the early peak in the trajectory, which aligns with the hypothesis. We also identified different peak ages for those regions, ranging from 24 to 41 years, suggesting that cognitive control regions do not develop at the same rate. Hence, the maturation of cognitive control occurs at distinct time points across various brain regions.

Previous research has indicated that the attentional orientation function is preserved during aging[37]. Consistently, we found that the dorsal attention network regions underlying the attentional orientation showed a relatively flat developmental pattern, in contrast to the inverted U-shaped trajectory in cognitive control network regions. The dissociation between these two sets of regions reflects hierarchical age effects on brain function. On the one hand, the brain regions are organized in a functional hierarchy, with the frontoparietal cognitive control network to be at the highest level. It acts as a connectivity hub, receiving inputs from and providing feedback to other systems, including the dorsal attention network[38]. During conflict tasks, the two sets of regions are coordinated in a hierarchical manner, with the cognitive control network maintaining task goals and executing conflict resolution, while the dorsal attention network directs attention towards task-relevant stimuli[39]. Even within the prefrontal cortex itself, a hierarchical organization exists, with middle frontal areas occupying the peak position[40]. These are in line with our finding that the

400 middle frontal cortex is dissociated from rostral and caudal frontal regions, and the
401 cognitive control network is dissociated from the dorsal attention network (Figure 4).
402 On the other hand, different brain regions exhibit different age effects. Higher-order
403 regions typically have more complex developmental trajectories[35] and reach their
404 peak maturation during later periods[32,41]. Specifically, prefrontal control regions are
405 among the last to mature and one of the earliest to decline[4,8,42]. Therefore, the
406 dissociation between cognitive control and dorsal attention regions likely reflects their
407 different positions within the functional hierarchy and the corresponding age-related
408 patterns of change.

409 Critically, there was no region showing higher activity in the elderly compared to
410 the young adults (see supplementary Note S1). Interestingly, we also observed a
411 noteworthy greater left laterality in elderly adults, contrary to the compensation
412 theory[43] and the hemispheric asymmetry reduction in older adults theory[44]. These
413 theories propose that elderly adults recruit additional brain regions in a more
414 symmetric manner to compensate for age-related cognitive decline. Stronger patterns
415 of left laterality were also identified in childhood, primarily driven by the prefrontal
416 region (Figure 5). The left laterality at both ends of the age spectrum reflects
417 differential age effects on the cerebral hemispheres. The left hemisphere is known to
418 undergo earlier development[45] and later decline[46] compared to the right hemisphere.
419 Consequently, a stronger imbalance in activity favoring the left hemisphere may occur
420 in both childhood and elderly adulthood. Notably, it is likely that previous studies
421 showing stronger laterality in young adults may have been biased by too small sample
422 sizes and the use of non-quantitative methods for calculation of laterality[47,48].
423 Moreover, since both left and right lateralized results were reported in the literature on
424 laterality[46], it is reasonable to observe a low laterality for the young adults in the
425 current meta-analysis.

426 By incorporating all the studies, our results demonstrate that the SDM has
427 relatively higher sensitivity than that of the ALE in identifying involved brain regions.

Moreover, the SDM also has the added advantage of fully utilizing existing effect size data and coordinates[49], allowing us to compare the relative activity strength among various age groups, such as the contrast between young adults and elderly groups. More importantly, this approach enables us to conduct meta-regressions to examine parametric relationships between brain region activity and age, thus providing developmental trajectories of cognitive control regions. Future studies could implement this approach to better link cognitive-behavioral measurements with brain functions.

One caveat to consider in this study is the non-uniform distribution of age among the included studies. Specifically, most of the young adult studies (71 out of 74) had average ages between 20 and 40, resulting in a noticeable gap in the age range of 41 to 55. While these studies may have recruited an adequate number of individuals within this age range, the focus on the mean age may limit our study to capture this variation. Consequently, it is important to acknowledge that the observed age distribution could potentially impact the results of the regression analysis. Another noteworthy caveat is the potential occurrence of ecological fallacy[50] when interpreting the results of meta-regression analyses. The ecological fallacy suggests that associations observed at the group level may not necessarily hold true for individuals within those groups. Therefore, while our analysis reveals significant associations between brain activities and age across various studies, it does not provide direct insights into the specific age effects at the individual level. Future research incorporating individual-level investigations (e.g., longitudinal follow-up studies) is crucial to obtaining a more comprehensive understanding of these relationships. Additionally, the disparity in brain activity levels between youth and young adults may be influenced by various physiological factors, such as differences in baseline glucose consumption, blood flow and amount of artifacts caused by motion, respiration, or cardiac activity.

Reference

1. Cohen, J.D. Cognitive control: Core constructs and current considerations. in *The Wiley handbook of cognitive control* (ed. T. Egner) 1-28 (2017).
2. Miller, E.K. & Cohen, J.D. An integrative theory of prefrontal cortex function. *Annu Rev Neurosci* **24**, 167-202 (2001).
3. Li, Z., Goschl, F. & Yang, G. Dissociated neural mechanisms of target and distractor processing facilitated by expectations. *J. Neurosci* **40**, 1997-1999 (2020).
4. Craik, F.I. & Bialystok, E. Cognition through the lifespan: mechanisms of change. *Trends Cogn Sci* **10**, 131-138 (2006).
5. Casey, B.J., Getz, S. & Galvan, A. The adolescent brain. *Dev Rev* **28**, 62-77 (2008).
6. Diamond, A. Executive functions. *Annu. Rev. Psychol* **64**, 135-168 (2013).
7. Zanto, T.P. & Gazzaley, A. Attention and Ageing. in *The Oxford Handbook of Attention* (ed. A.C. Nobre & S. Kastner) 0 (Oxford University Press, 2014).
8. Casey, B.J., Tottenham, N., Liston, C. & Durston, S. Imaging the developing brain: what have we learned about cognitive development? *Trends Cogn Sci* **9**, 104-110 (2005).
9. Grady, C. The cognitive neuroscience of ageing. *Nat Rev Neurosci* **13**, 491-505 (2012).
10. Ferguson, H.J., Brunsdon, V.E.A. & Bradford, E.E.F. The developmental trajectories of executive function from adolescence to old age. *Sci Rep* **11**, 1382 (2021).
11. De Luca, C.R. & Leventer, R.J. Developmental trajectories of executive functions across the lifespan. in *Executive functions and the frontal lobes* 57-90 (Psychology Press, 2010).
12. Li, S.C., Hammerer, D., Muller, V., Hommel, B. & Lindenberger, U. Lifespan development of stimulus-response conflict cost: similarities and differences between maturation and senescence. *Psychol Res* **73**, 777-785 (2009).
13. Brouwer, R.M., *et al.* Genetic variants associated with longitudinal changes in brain structure across the lifespan. *Nat Neurosci* **25**, 421-432 (2022).
14. Bethlehem, R.A.I., *et al.* Brain charts for the human lifespan. *Nature* **604**, 525-533 (2022).
15. Li, Q., *et al.* Conflict detection and resolution rely on a combination of common and distinct cognitive control networks. *Neurosci Biobehav Rev* **83**, 123-131 (2017).
16. Giedd, J.N., *et al.* Brain development during childhood and adolescence: a longitudinal MRI study. *Nat Neurosci* **2**, 861-863 (1999).
17. Rubia, K. Functional brain imaging across development. *Eur Child Adolesc Psychiatry* **22**, 719-731 (2013).

18. Bunge, S.A., Dudukovic, N.M., Thomason, M.E., Vaidya, C.J. & Gabrieli, J.D. Immature frontal lobe contributions to cognitive control in children: evidence from fMRI. *Neuron* **33**, 301-311 (2002).
19. Milham, M.P.*, et al.* Attentional control in the aging brain: insights from an fMRI study of the stroop task. *Brain Cogn* **49**, 277-296 (2002).
20. Yaple, Z.A., Stevens, W.D. & Arsalidou, M. Meta-analyses of the n-back working memory task: fMRI evidence of age-related changes in prefrontal cortex involvement across the adult lifespan. *Neuroimage* **196**, 16-31 (2019).
21. Fernandez, N.B., Hars, M., Trombetti, A. & Vuilleumier, P. Age-related changes in attention control and their relationship with gait performance in older adults with high risk of falls. *Neuroimage* **189**, 551-559 (2019).
22. Sebastian, A.*, et al.* Differential effects of age on subcomponents of response inhibition. *Neurobiology of aging* **34**, 2183-2193 (2013).
23. Hart, H., Radua, J., Nakao, T., Mataix-Cols, D. & Rubia, K. Meta-analysis of functional magnetic resonance imaging studies of inhibition and attention in attention-deficit/hyperactivity disorder: exploring task-specific, stimulant medication, and age effects. *JAMA psychiatry* **70**, 185-198 (2013).
24. Zhang, Z.*, et al.* Neural substrates of the executive function construct, age-related changes, and task materials in adolescents and adults: ALE meta-analyses of 408 fMRI studies. *Dev Sci* **24**, e13111 (2021).
25. Long, J.*, et al.* Distinct neural activation patterns of age in subcomponents of inhibitory control: A fMRI meta-analysis. *Front Aging Neurosci* **14**, 938789 (2022).
26. Nee, D.E., Wager, T.D. & Jonides, J. Interference resolution: insights from a meta-analysis of neuroimaging tasks. *Cognitive, affective & behavioral neuroscience* **7**, 1-17 (2007).
27. Zuo, X.N.*, et al.* Growing together and growing apart: regional and sex differences in the lifespan developmental trajectories of functional homotopy. *J Neurosci* **30**, 15034-15043 (2010).
28. Coupe, P., Catheline, G., Lanuza, E., Manjon, J.V. & Alzheimer's Disease Neuroimaging, I. Towards a unified analysis of brain maturation and aging across the entire lifespan: A MRI analysis. *Hum Brain Mapp* **38**, 5501-5518 (2017).
29. Amlien, I.K., Sneve, M.H., Vidal-Pineiro, D., Walhovd, K.B. & Fjell, A.M. The Lifespan Trajectory of the Encoding-Retrieval Flip: A Multimodal Examination of Medial Parietal Cortex Contributions to Episodic Memory. *J Neurosci* **38**, 8666-8679 (2018).
30. Yeo, B.T.*, et al.* The organization of the human cerebral cortex estimated by intrinsic functional connectivity. *J Neurophysiol* **106**, 1125-1165 (2011).
31. Yarkoni, T., Poldrack, R.A., Nichols, T.E., Van Essen, D.C. & Wager, T.D. Large-scale automated synthesis of human functional neuroimaging data. *Nat Methods* **8**, 665-670 (2011).

538 32. Gogtay, N., *et al.* Dynamic mapping of human cortical development during
539 childhood through early adulthood. *Proc Natl Acad Sci U S A* **101**, 8174-8179
540 (2004).
541 33. Luna, B., Marek, S., Larsen, B., Tervo-Clemmens, B. & Chahal, R. An
542 integrative model of the maturation of cognitive control. *Annu Rev Neurosci* **38**,
543 151-170 (2015).
544 34. Brenhouse, H.C. & Andersen, S.L. Developmental trajectories during
545 adolescence in males and females: a cross-species understanding of underlying
546 brain changes. *Neurosci Biobehav Rev* **35**, 1687-1703 (2011).
547 35. Shaw, P., *et al.* Neurodevelopmental trajectories of the human cerebral cortex. *J*
548 *Neurosci* **28**, 3586-3594 (2008).
549 36. Grimm, K.J., Ram, N. & Estabrook, R. *Growth Modeling: Structural Equation*
550 *and Multilevel Modeling Approaches* (Guilford Publications, 2016).
551 37. Verissimo, J., Verhaeghen, P., Goldman, N., Weinstein, M. & Ullman, M.T.
552 Evidence that ageing yields improvements as well as declines across attention
553 and executive functions. *Nat Hum Behav* **6**, 97-110 (2022).
554 38. Cole, M.W., *et al.* Multi-task connectivity reveals flexible hubs for adaptive task
555 control. *Nat Neurosci* **16**, 1348-1355 (2013).
556 39. Petersen, S.E. & Posner, M.I. The attention system of the human brain: 20 years
557 after. *Annu Rev Neurosci* **35**, 73-89 (2012).
558 40. Badre, D. & Nee, D.E. Frontal Cortex and the Hierarchical Control of Behavior.
559 *Trends Cogn Sci* **22**, 170-188 (2018).
560 41. Sydnor, V.J., *et al.* Intrinsic activity development unfolds along a
561 sensorimotor-association cortical axis in youth. *Nat Neurosci* **26**, 638-649
562 (2023).
563 42. Raz, N., *et al.* Selective aging of the human cerebral cortex observed in vivo:
564 differential vulnerability of the prefrontal gray matter. *Cereb Cortex* **7**, 268-282
565 (1997).
566 43. Reuter-Lorenz, P.A. & Cappell, K.A. Neurocognitive aging and the
567 compensation hypothesis. *Current Directions in Psychological Science* **17**,
568 177-182 (2008).
569 44. Cabeza, R. Hemispheric asymmetry reduction in older adults: the HAROLD
570 model. *Psychol Aging* **17**, 85-100 (2002).
571 45. Thatcher, R.W., Walker, R.A. & Giudice, S. Human cerebral hemispheres
572 develop at different rates and ages. *Science* **236**, 1110-1113 (1987).
573 46. Dolcos, F., Rice, H.J. & Cabeza, R. Hemispheric asymmetry and aging: right
574 hemisphere decline or asymmetry reduction. *Neurosci Biobehav Rev* **26**, 819-825
575 (2002).
576 47. Cabeza, R., *et al.* Age-related differences in neural activity during memory
577 encoding and retrieval: a positron emission tomography study. *J Neurosci* **17**,
578 391-400 (1997).

48. Grady, C.L., Bernstein, L.J., Beig, S. & Siegenthaler, A.L. The effects of encoding task on age-related differences in the functional neuroanatomy of face memory. *Psychol Aging* **17**, 7-23 (2002).
49. Albajes-Eizagirre, A., Solanes, A., Vieta, E. & Radua, J. Voxel-based meta-analysis via permutation of subject images (PSI): Theory and implementation for SDM. *Neuroimage* **186**, 174-184 (2019).
50. Thompson, S.G. & Higgins, J.P. How should meta-regression analyses be undertaken and interpreted? *Stat Med* **21**, 1559-1573 (2002).

Methods

Literature preparation

Literature Search

We first searched articles on the youth and the elderly from PUBMED and Web of Science till 2022. The following search terms were applied in titles, abstracts, table of contents, indexing, and key concepts: *("Stroop" OR "Flanker" OR "Simon" OR "SNARC" OR "Navon" OR "interference" OR "cognitive conflict") AND ("fMRI" OR "functional resonance imaging" OR "functional imaging" OR "neuroimaging" OR "PET") AND ("children" OR "kids" OR "adolescents" OR "teenagers" OR "underage" OR "aged" OR "old" OR "older" OR "elder" OR "elderly" OR "senior" OR "development" OR "developmental" OR "aging" OR "life span").* The above process yielded 3,388 articles. Besides, 111 studies on the young adult from a previous meta-analysis study[15] were adopted, which had applied very similar recruitment criteria. Moreover, we screened 8 articles citing or being cited by the crucial literature. After removing 681 duplicates, the literature search identified 2,826 articles.

Exclusion Criteria

We excluded any articles that met one or more of the following predefined exclusion criteria: 1) not in English; 2) not including healthy human participants; 3) case study; 4) not empirical study; 5) not functional resonance imaging (fMRI) or positron emission tomography (PET) study; 6) not whole-brain results (i.e., not have covered the whole gray matter); 7) not in Talairach or Montreal Neurological Institute (MNI) space; 8) not reflecting the congruency effect (i.e., contrasts between incongruent and congruent or between incongruent and neutral conditions); 9) not reporting exact mean age of participants.

A total of 107 articles were identified as eligible for inclusion in our meta-analyses. Supplementary Figure S1 shows the preferred reporting items for systematic reviews and meta-analyses (PRISMA)[51] flow chart for the literature screening process. The 107 articles included 113 experiments (individual contrasts reported in the articles) with 3,153 participants and 1,428 activation foci reported. None of the experiments share the same group of participants.

Coding Procedure

A coding manual was formulated to record pertinent study information, including authors, publication dates, experimental tasks, contrasts, and sample demographics (such as the average age and sample size). To ensure coding accuracy, two authors (ZL and GY) independently coded all studies, with discrepancies resolved through discussion or reference to the original studies. In instances where studies lacked essential information, such as peak coordinates for relevant contrasts, participant age averages, or data for specific age groups, efforts were made to contact the authors via e-mail to obtain the relevant data. In addition, both coordinates and effect sizes (i.e., Hedge's *g*) were extracted from each study. Further, Talairach space coordinates were transformed to MNI coordinates using the Lancaster transform[52].

Meta-Analytic Procedure

Activation likelihood estimation (ALE)

In order to obtain a comprehensive understanding of cognitive control-related brain activity across all age groups and to replicate our prior study[15], we initially conducted a single dataset meta-analysis using BrainMap GingerALE software[53] (version 3.0.2, http://www.brainmap.org). This meta-analytical approach, known as activation likelihood estimation, utilizes the spatial convergence of brain activity across multiple studies to determine the probability of activation in specific regions. Foci from

638 individual studies were transformed into a standardized coordinate space and modeled
639 as Gaussian probability values that accounted for variability in the number of
640 participants in each study. In situations where foci overlapped across studies, multiple
641 Gaussians were associated with a single focus, and ALE selected the Gaussian with
642 maximum probability for each focus[54]. Subsequently, ALE score maps were
643 generated by comparing these modeled Gaussian distributions with a null distribution
644 that simulated random brain effects. The null distribution was generated using the
645 same sample size and number of foci groups as the experimental dataset for 10,000
646 times[53]. ALE scores were then used to calculate *p*-values, which were based on the
647 proportion of values higher than a certain threshold in the null distribution. This
648 resulted in a statistical ALE map that differentiated true brain effects from random
649 effects. A cluster-defining threshold of $p < 0.001$ and a minimum cluster size of 10
650 voxels (80 mm^3) were utilized to compute ALE maps, which matches the threshold
651 applied in the seed-based *d* mapping (SDM) approach (see below).

652 **Seed-based effect size mapping**

653 SDM is an alternative approach to statistically synthesize results from multiple fMRI
654 experiments[49]. Similar to ALE, SDM employs a coordinate-based random-effects
655 approach to amalgamate peak coordinate information into a standard space across
656 several experiments. However, while ALE solely considers the binary feature (i.e.,
657 active versus inactive) of peak coordinates, SDM takes into account the quantitative
658 effect size (can be positive or negative) connected to each peak and reconstructs the
659 initial parametric maps of individual experiments before amalgamating them into a
660 meta-analytic map[55]. Therefore, the use of a distinct algorithm in SDM from ALE
661 allows us to scrutinize the robustness and replicability of the outcomes obtained via
662 ALE. More importantly, SDM enables the inclusion of covariates in the
663 meta-regression analyses to reflect the changes in brain function across the lifespan.

664 We conducted three types of analyses using the SDM approach. Firstly, we

665 estimated the mean activation across all age groups and compared the results with
666 ALE's single dataset meta-analysis results. Secondly, we conducted a contrast
667 between two groups of studies (e.g., between young adults and that of the non-young
668 adults, i.e., combining youth and elderly groups) to identify brain regions that showed
669 different levels of activity. Thirdly, we defined specific models (e.g., quadratic and
670 square root models) to fit the whole brain to validate brain regions adhering to the
671 hypothetical developmental patterns (e.g., inverted U-shaped).

672 These analyses were conducted using the SDM-PSI software (version 6.22,
673 https://www.sdmproject.com). Effect size maps were built for the 113 individual
674 experiments. This was accomplished by (a) converting the statistical value of each
675 peak coordinate into an estimate of effect size (Hedge's *g*) using standard formulas[56]
676 and (b) convolving these peaks with a fully anisotropic unnormalized Gaussian kernel
677 ($\alpha = 1$, FWHM = 20 mm) within the boundaries of a gray matter template (voxel size
678 = 2×2×2 mm^3). Imputation (50 times) was conducted for each study separately to
679 obtain an reliable estimate of brain activation maps[55]. Besides, the individual effect
680 size maps were combined using a random-effect general linear model. To assess the
681 statistical significance of activations in the resulting meta-analytic effect size map,
682 1,000 random permutations of activation peaks within the gray matter template were
683 compared. Finally, the meta-analytic maps were thresholded using a voxel-wise
684 family-wise error (FWE) corrected threshold of $p < 0.001$ and a cluster-wise extent
685 threshold of 10 voxels[57].

686 *Mean analyses across all studies*

687 This analysis aimed to characterize the activation patterns of cognitive control-related
688 brain regions across all studies, which was conducted utilizing the "Mean" function in
689 SDM-PSI software. In order to verify the reliability of the SDM analysis results, we
690 compared the results with the single dataset meta-analyses using ALE.

691 *Contrast analyses*

692 To test our hypothesis that cognitive control related brain activities develop in an
693 inverted U-shaped trajectory with age, we categorized each study based on the mean
694 age of participants into a youth group (8−18 years), young adults group (20−44 years),
695 and elderly group (54−74 years). The age boundaries were determined to minimize
696 age distribution overlap. We utilized SDM-PSI to perform a contrast analysis between
697 the group of young adults and the other two groups, in order to fully identify potential
698 brain regions that exhibit an inverted U-shaped developmental trajectory. This was
699 achieved by assigning studies from the adult group as 1 and all other studies as −1.
700 This analysis yielded two results, one showing higher activity in young adults than the
701 youth and elderly groups, and the other showing the opposite. Results from this
702 analysis were used as regions of interest (ROIs) in the subsequent model fitting
703 analyses (see sections "Generalized additive model (GAM) fitting" and "Model
704 simplification and model comparison"). The possibility of publication bias for
705 resultant clusters was examined using Egger's test[58], in which any result showing $p <$
706 0.05 was regarded as having significant publication bias. Heterogeneity was evaluated
707 using the I^2 index, which quantifies the proportion of total variability attributable to
708 heterogeneity between studies. A value less than 25% indicates low heterogeneity
709 among the included studies[59]. In addition, to further test our specific interest between
710 elderly group and young adult group, we conducted a contrast by assigning young
711 adults as 1 and elderly adults as −1, without including the youth group (see
712 supplementary Note S1).

713 *Meta-regression analyses*

714 To better describe the possible developmental trajectories of the whole brain, we
715 carried out meta-regression analyses with the age and/or its derivatives as regressors.
716 In total three regressions were conducted across the whole-brain, including a linear

717 regression (with only age as the regressor), a quadratic regression (with age and its
718 square as separate regressors) and a square root regression (with age and its square
719 root as separate regressors). The linear regression aimed to test regions with
720 increasing/decreasing activity with age (see supplementary Note S1), and the other
721 two non-linear regressions aimed to test regions with the inverted U-shaped
722 trajectories based on the model fitting results.

723 Masks were generated for each peak coordinate derived from the contrast
724 analyses described above. These masks were centered at the peaks and comprised of 8
725 voxels. Subsequently, we extracted the effect sizes for each mask. Fifty values were
726 obtained from the SDM iterations and subsequently averaged for each study in each
727 region. The iterated variances were also averaged in a similar way. Additionally, we
728 removed the outliers (beyond 3 standard deviations from the mean) in the following
729 model fitting analyses.

730 **Generalized additive model (GAM) fitting**

731 To precisely estimate the inverted U-shaped trajectories, we adopted the GAM to fit
732 the curves. The GAM allows for flexible, nonparametric smoothing of predictor
733 variables[60], and has been widely used to depict the developmental trajectories[14,61]. We
734 implemented GAMs using the "mgcv" package[62] in R. For each ROI, we fitted a
735 GAM with the following formula:

736 $$g \sim s(age),$$

737 where g is the effect size (dependent variable), and s(age) represents a smoothing
738 spline of age (predictor variable). We also adjusted the estimate with a weight
739 parameter, which was the reciprocal of variance. We used penalized regression splines,
740 with the amount of smoothing determined automatically based on generalized cross
741 validation.

For each ROI, we quantified the peak age by choosing the highest prediction of a fine-grained age scale (1000 points from 8 to 74 years old). We also calculated the estimated degree of freedom (EDF) for the smooth curve by summing up the degree of freedom for each penalized term (i.e., s(age).1 to s(age).9).

Model simplification and model comparison

While the GAM analysis may yield good fitting results on the data, it is important to acknowledge its potential drawbacks. One concern is that it can fit the data with a high degree of freedoms (up to 7.1, supplementary Table S4), which makes it susceptible to over-fitting and harder to generalize. Another issue is its poor interpretability. Therefore, we next sought to fit the data with simpler models.

To this end, we used the "metafor" package in R to fit these effect sizes with the age and its derivatives as predictors. Specifically, we tested four non-linear models (see below). Quadratic and cubic models were included based on previous studies[27-29]; quadratic logarithmic and square-root models were included to capture the possible skewed trajectory, which would reflect the asymmetric trajectory of development and decline of cognitive control[4]. Each model was fitted to each ROI separately. We calculated the Akaike information criterion (AIC) to evaluate the goodness of fit for each model.

1) Quadratic model
   $g \sim \text{age} + \text{age}^2$
2) Cubic model
   $g \sim \text{age} + \text{age}^2 + \text{age}^3$
3) Quadratic logarithmic model
   $g \sim \log(\text{age}) + (\log(\text{age}))^2$
4) Square root model
   $g \sim \text{age} + \text{sqrt}(\text{age})$

768 **Neurosynth decoding analysis**

769 To investigate the potential functional difference between the two sets of brain
770 regions reported in section "Dissociated brain networks with distinct developmental
771 trajectory", we generated two binary maps from the contrast analysis between young
772 adults and other groups, and then submitted them to the NeuroSynth decoding
773 system[31]. The inverted and non-inverted U-shaped maps were obtained by applying
774 thresholds of $p < 0.05$, and $p > 0.1$, respectively. These lenient threshold boundaries
775 were used to minimize the impact of sparsity on the decoding results. Additionally, to
776 focus on the brain regions specifically related to cognitive control, the two maps were
777 masked by using results from the mean SDM analysis (see section "Regions related to
778 cognitive control identified by both ALE and SDM" in Results). In the decoding
779 results, we deleted terms that were related to brain regions (e.g., "frontal"), not
780 functional specific (e.g., "task"), and duplicated (e.g., "attention" was removed if
781 there was already "attentional").

782 **Laterality analysis**

783 We calculated the laterality based on the effect size of reported brain coordinates from
784 each study. We computed the sum of effect sizes across coordinates for left and right
785 hemisphere, respectively, yielding one global effect size each (i.e., g_L and g_R). Then,
786 we calculated the index of brain laterality with the following equation[63]:

787 $$\text{laterality} = \frac{g_L - g_R}{g_L + g_R},$$

788 which was then submitted to the GAM and simplified models (i.e., the quadratic,
789 cubic, square root, and quadratic logarithmic models).

790 To illustrate the contribution of different brain regions to the age effect of
791 laterality, we calculated the laterality for each voxel[64]. We first used the SDM-PSI to
792 conduct a mean analysis for each age group (i.e., the youth, young adult and elderly),

yielding three z-maps. Then the laterality was computed with the above equation for each voxel from the left hemisphere. The opposite values were calculated for the right hemisphere. To avoid the bias due to asymmetric brain hemispheres, we removed voxels without corresponding mirror coordinates. The results were visualized confining to the brain regions estimated from the grand mean analyses (see section "Seed-based effect size mapping" in Results).

Data availability

The data used for this meta-analysis are publicly available. The sources of the data are listed in the supplementary Table S1. Additionally, the raw data extracted from the included articles and the intermediate data used to produce the results can be accessed from https://github.com/guochun-yang/Cognitive_Control_Developmental_Trajectory/.

Code availability

The whole-brain analyses (including the grand mean analyses, the contrast analyses and meta-regressions) were performed with the publicly available softwares, including the GingerALE (version 3.0.2, https://www.brainmap.org) and SDM-PSI (version 6.22, https://www.sdmproject.com). The analyses with intermediate data, such as regions-of-interest-based data extracted from the whole-brain results, were performed with the R software in Rstudio (version 2023.06.0, https://posit.co/products/open-source/rstudio), and the codes can be accessed from https://github.com/guochun-yang/Cognitive_Control_Developmental_Trajectory/.

Reference

51. Page, M.J., *et al.* The PRISMA 2020 statement: an updated guideline for reporting systematic reviews. *BMJ* **88**, 105906 (2021).
52. Lancaster, J.L., *et al.* Bias between MNI and talairach coordinates analyzed using the ICBM-152 brain template. *Human Brain Mapping* **28**, 1194-1205 (2007).
53. Eickhoff, S.B., Bzdok, D., Laird, A.R., Kurth, F. & Fox, P.T. Activation likelihood estimation meta-analysis revisited. *Neuroimage* **59**, 2349-2361 (2012).
54. Turkeltaub, P.E., *et al.* Minimizing within-experiment and within-group effects in activation likelihood estimation meta-analyses. *Human Brain Mapping* **33**, 1-13 (2012).
55. Radua, J. & Mataix-Cols, D. Meta-analytic methods for neuroimaging data explained. *Biol Mood Anxiety Disord* **2**, 6 (2012).
56. Hedges, L.V. Distribution theory for Glass's estimator of effect size and related estimators. *Journal of Educational Statistics* **6**, 107-128 (1981).
57. Radua, J., *et al.* A new meta-analytic method for neuroimaging studies that combines reported peak coordinates and statistical parametric maps. *Eur Psychiat* **27**, 605-611 (2012).
58. Egger, M., Smith, G.D. & Phillips, A.N. Meta-analysis: principles and procedures. *BMJ* **315**, 1533–1537 (1997).
59. Higgins, J.P.T., Thompson, S.G., Deeks, J.J. & Altman, D.G. Measuring inconsistency in meta-analyses. *BMJ* **327**, 557-560 (2003).
60. Wood, S.N. *Generalized additive models: an introduction with R* (CRC press, 2017).
61. Zuo, X.N., *et al.* Human Connectomics across the Life Span. *Trends Cogn Sci* **21**, 32-45 (2017).
62. Wood, S.N. mgcv: GAMs and generalized ridge regression for R. *J R news* **1**, 20-25 (2001).
63. Seghier, M.L. Laterality index in functional MRI: methodological issues. *Magn Reson Imaging* **26**, 594-601 (2008).
64. Hoffman, P. & Morcom, A.M. Age-related changes in the neural networks supporting semantic cognition: A meta-analysis of 47 functional neuroimaging studies. *Neurosci Biobehav Rev* **84**, 134-150 (2018).

Table 1. Brain areas activated in the contrast analysis (voxel-wise FWE-corrected, $p < 0.001$, with minimum cluster size ≥ 10 voxels) with the SDM-PSI.

Order	# Voxels	*Z*	*p*	L/R	MNI coordinate			Anatomical location	BA
					x	y	z		
1	1196	5.115	< 0.001	R	52	16	4	inferior frontal gyrus	48
2	677	4.484	< 0.001	R	54	−48	40	inferior parietal lobule	40
3	658	5.281	< 0.001	L	−44	16	24	inferior frontal gyrus	48
4	243	3.818	< 0.001	R	10	4	6	caudate nucleus	/
5	229	3.294	< 0.001	L	−8	0	64	pre-supplementary motor area	6
6	145	3.524	< 0.001	L	−36	−50	44	superior parietal lobule	40
7	85	3.194	< 0.001	L	−38	24	−4	anterior insula	47
8	59	3.249	< 0.001	L	−8	10	4	caudate nucleus	/
9	49	3.355	< 0.001	L	−10	−64	60	precuneus	7
10	47	3.059	< 0.001	L	−36	12	−6	posterior insula	48
11	36	3.459	< 0.001	L	−10	−20	2	anterior thalamic projections	/
12	33	3.133	< 0.001	R	50	−64	4	middle temporal gyrus	37
13	16	2.917	< 0.001	L	−30	−68	−20	cerebellum	19
14	13	2.767	< 0.001	L	−60	−36	30	supramarginal gyrus	40
15	10	2.972	< 0.001	L	−58	−44	22	superior temporal gyrus	42

Note. The orders in the table correspond to the numbers of each plot in Figure 2. ALE = activation likelihood estimation; MNI = Montreal Neurological Institute; BA = Brodmann area; L = left; R = right.

Acknowledgement

We thank Fergus I.M. Craik and Beatriz Luna for valuable suggestions on a previous version of this manuscript. We also thank Jing Yang and Yifan Zhang for the data check of extracted coordinates. Z.L. discloses support for the research of this work from Scientific Research Fund of Zhejiang Provincial Education Department (Y202249966) and Starting Research Fund from Hangzhou Normal University (2021QDL079). I.T.P discloses support for the research of this work from the Eunice Kennedy Shriver National Institute of Child Health and Human Development (NICHD) (HD098235). G.Y. disclose support for the research of this work from Jiefeng Jiang, and China Postdoctoral Science Foundation (2019M650884). X.L. discloses support for the research of this work from the Ministry of Science and Technology of the People's Republic of China (2021ZD0200505).

Author contributions

Conceptualization: Z.L. and G.Y.; Methodology: Z.L. and G.Y.; Formal analysis: Z.L. and G.Y.; Data curation: Z.L. and G.Y.; Writing original draft: Z.L. and G.Y.; Writing, review, and editing: Z.L., I.T.P., J.R., L.W., X.L. and G.Y.; Funding: Z.L., I.T.P., X.L. and G.Y; Supervision: G.Y.

Competing interests

The authors declare no competing interests.

Inclusion & ethics

All collaborators of this study fulfilled the criteria for authorship required by Nature Portfolio journals have been included as authors, as their participation was essential for implementation of the study and improvement of the manuscript. Roles and

responsibilities were agreed among collaborators ahead of the research. This work does not include findings that are locally relevant. As a meta-analysis, this study does not involve direct interactions with human participants or the collection of new data. Each of the original studies included in this meta-analysis obtained ethical approval from their respective institutions, and we confirm that we complied with all applicable ethical guidelines and regulations.